

Multicomponent control via shaped, strong laser fields mass spectrometry

LALINDA PALLIYAGURU[†], JOSEPH SLOSS[†],
HERSCHEL RABITZ[‡] and ROBERT J. LEVIS^{*†}

[†]Center for Advanced Photonics Research and Department of Chemistry,
Temple University, Philadelphia, PA 19122, USA

[‡]Department of Chemistry, Princeton University, Princeton,
NJ 08544, USA

(Received 28 February 2007; in final form 19 March 2007)

The fragmentation processes of polyatomic molecules induced by an intense laser field exhibit sensitive dependence on the laser characteristics such as intensity, pulse duration, wavelength, and shape of the temporal pulse envelope. Adaptive laser pulse shaping can control the fragmentation of methyl/methoxy groups in dimethyl methylphosphonate (DMMP), a simulant for nerve agent sarin. The exploitation of the sensitivity of molecular fragmentation to laser pulse shapes represents a new way to discriminate molecular identity. Here we have shown manipulation of branching ratio $M-(OCH_3)^+/M-(CH_3)^+$, $M-2(CH_3)^+/M-(CH_3)^+$ and $M-(OCH_3)^+/M-2(CH_3)^+$ fragment ion ratios for DMMP in the presence of complex background in the extraction region of a TOF spectrometer using tailored femtosecond laser pulses. We suggest that the use of adaptive femtosecond laser pulse shaping coupled to TOF mass spectrometry is an accurate way to identify complex airborne organophosphate molecules similar to nerve agents.

1. Introduction

The development of rapid and reliable methods for the detection of polyatomic molecules such as chemical warfare (CW) agents is challenging given the large variety of chemical functionality in potential target molecules [1–3]. Functionality including phospho, fluorine, thiol and cyanide groups are found, for example, in the lethal CW agents sarin, tabun and soman, the powerful inhibitors for the enzyme acetylcholinesterase [4].

Ion mobility spectrometry [5] is widely used for the detection of nerve gases, despite problematic false positive/false negative response in the presence of ‘matrix effects’ such as hydrocarbon, humidity, and interferents in the environment.

*Corresponding author. Email: rjlevis@temple.edu

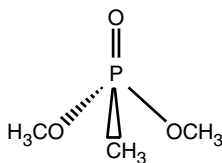


Figure 1. The chemical structure of dimethyl methylphosphonate.

Other detection methods including the surface acoustic wave (SAW) [6, 7], potentiometric [8], enzymatic assay [9, 10], porous silicon interferometric [11] and chemosensor [12] devices are under investigation as potential detection systems, each also has many problematic interferents. Any useful detection system must have high sensitivity and selectivity for agents in the presence of interfering compounds to avoid false negative/positive responses.

Mass spectrometry (MS) has been coupled to other analytical techniques such as gas chromatography (GC-MS) [13–15], liquid chromatography (LC-MS) [16, 17], and ion mobility spectrometry (IMS-MS) [18, 19] for the detection of chemical nerve agent in the presence of background. The detection scheme is based on two steps, first, the separation of nerve agents based on retention index or ion mobility constant, second, the analysis of the mass spectrum obtained with chemical or electron impact ionization mass spectrometry [20, 21]. There are major limitations associated with these techniques, such as the chemical noise produced by hydrocarbon content, and low detector sensitivity to organophosphates [22, 23].

Rather than using a pre-separation technique, we demonstrate the ability to directly manipulate the time-of-flight (TOF) mass spectral fragmentation pattern of dimethyl methylphosphonate (DMMP) (figure 1), a simulant for the nerve agent sarin. DMMP is investigated in a mixture of hydrocarbon and water vapour using laser pulse shaping methods for discrimination. The hydrocarbon content of the mixture is composed of toluene, ethylbenzene and naphthalene creating a significant interference around the DMMP fragment ion features in the TOF mass spectrum. Strong field excitation using an intense ($10^{13} \text{ W cm}^{-2}$) $800 \pm 10 \text{ nm}$ laser pulse of molecules is one key to generating a variable mass spectral product distribution and has recently been an active area of research [24]. The strong field regime is reached at laser intensities in excess of $10^{12} \text{ W cm}^{-2}$, where electric field strengths is on the order of the binding fields of the valence electrons to nuclei. At these high intensities, the molecular potential energy surfaces are substantially modified and manipulation of molecular fragmentation dynamics and subsequent mass spectral product distribution become feasible [25, 26]. A number of product channels are accessible with strong field excitation leading to rich mass spectral product distribution. The second key is laser pulse shaping [27, 28] to manipulate molecular dissociation dynamics [29, 30]. The ability to manipulate the branching ratios of $M-(\text{OCH}_3)^+/M-(\text{CH}_3)^+$, $M-2(\text{CH}_3)^+/M-(\text{CH}_3)^+$, and $M-(\text{OCH}_3)^+/M-2(\text{CH}_3)^+$ of DMMP using shaped femtosecond laser pulses produces a new fingerprint method for the detection of a target simulant for chemical agents.

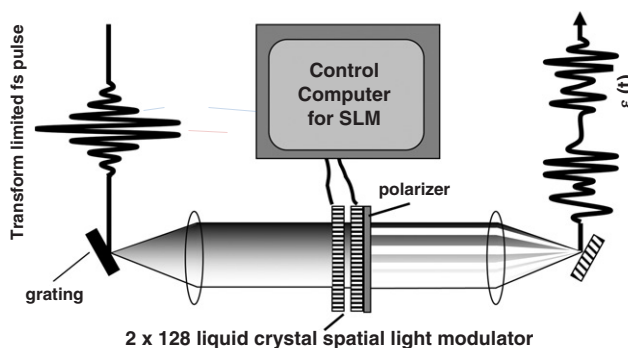


Figure 2. Schematic of the optical setup for generating a shaped laser pulse.

2. Experimental

The photonic reagents used to manipulate the mass spectra are synthesized from regeneratively amplified Ti:sapphire laser pulses at a repetition rate of 1 kHz. The pulse duration before shaping is 60 fs with a phase-locked bandwidth of 20 nm and energy of 1.2 mJ. The pulse shaper (figure 2) consists of a pair of diffraction gratings and lenses, arranged in a ‘zero dispersion pulse compressor’ configuration and a pulse-shaping mask (SLM). The individual frequency components contained within the input pulse are angularly dispersed by the first diffraction grating, and then focused to small diffraction limited lines at the back focal plane of the first cylindrical lens, where the frequency components are spatially separated along one dimension. Spatially patterned amplitude and phase masks are in this plane in order to manipulate the spatially dispersed frequency components. The second cylindrical lens and diffraction grating recombine all the frequencies into a single collimated beam to construct the shaped output pulse [30].

Spatial light modulation can produce a virtually unlimited number of different shaped laser pulses upon the transmission of the laser beam through the liquid crystal modulator [30]. The number of achievable pulse shapes is astronomically large ($>10^{200}$). To search this space an evolutionary algorithm [31, 32] is used to determine the optimal pulse shape based on feedback from experimental measurement (figure 3). A population of 40 random laser pulses (individuals) compose the members of the first generation where each member has a genome specified by the phases and amplitudes for the various frequency bands. A combination of crossover, mutation and cloning of the genomes of the members of the population are used to create subsequent generations. This evolutionary process eventually optimizes a pulse shape for the desired mass spectral fragmentation distribution. To obtain a representative mass spectrum we plot the average of the 40 different mass spectra produced by 40 different pulses in any generation.

Samples of DMMP, naphthalene, water, and a mixture of organic solvents (toluene and ethylbenzene in 1:1 ratio) were introduced into the TOF chamber by two independent precision variable leak valves to control the amount of each sample

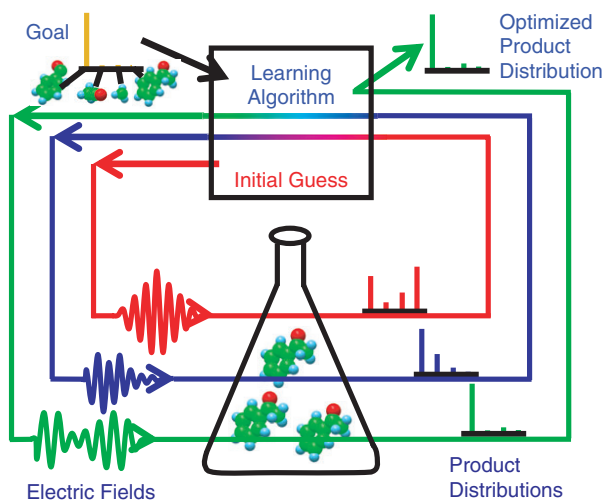


Figure 3. Representation of the concept of closed-loop control. In this case there are four possible outcomes shown for the interaction of the laser pulse with molecule. The desired distribution of the products is first input into the algorithm at the upper left of the figure. The program creates an initial laser pulse shape that interacts with the sample and yields a product distribution. Based on experimental measurement of the distribution (typical in combination with several other experiments) the algorithm creates a new pulse that yields a new distribution. The system loops iteratively until the desired level of control is exerted. (The colour version of this figure is included in the online version of the journal.)

introduced to the chamber. One leak valve regulated a mixture of organic solvents and water, in the TOF chamber to a pressure of 5.5×10^{-7} torr. The mole fractions of the solvents were adjusted to provide equal ion signals. The second leak valve regulated the pressure of the lower volatility samples of DMMP and naphthalene. The total pressure of the chamber with all five chemicals was 1.7×10^{-5} torr. The TOF chamber had a base pressure of 9.0×10^{-8} torr.

The laser was focused to a $100 \mu\text{m}$ spot in the extraction region of a time-of-flight mass spectrometer to induce both dissociation and ionization.

3. Results and discussion

We focus in this paper on controlling mass spectral branching ratios corresponding to the loss of methyl/methoxy group/s in DMMP by manipulating the shape of an intense laser pulse interacting with the molecule. After excitation of DMMP by an intense ($10^{13} \text{ W cm}^{-2}$) ultrafast (60 fs) laser pulse, the loss of functional groups give rise to features in the TOF mass spectrum, as shown in figure 4. We will concentrate on the peaks, $\text{M}-(\text{CH}_3)^+$ ($m/z = 109$), $\text{M}-2(\text{CH}_3)^+$ ($m/z = 94$), and $\text{M}-(\text{OCH}_3)^+$ ($m/z = 93$) as marked with asterisks to demonstrate the controllability of the fragmentation distribution using shaped laser pulses. The background molecules occupy about 50% of the sample volume resulting in high background signals in the TOF mass spectrum as shown in figure 5(a). The parent ion peaks of toluene and

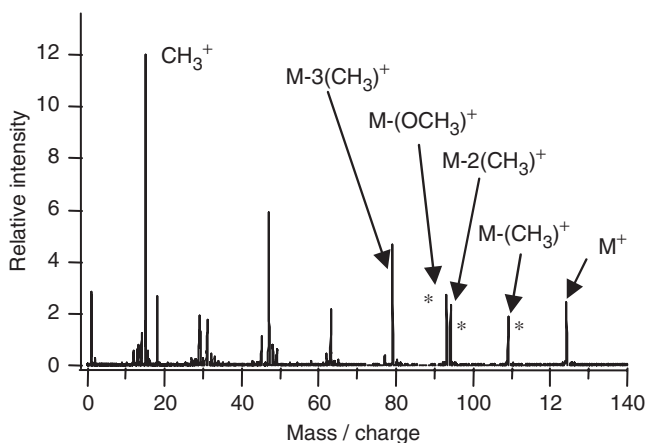


Figure 4. The time-of-flight mass spectra for the molecule dimethyl methylphosphonate after excitation using a transform-limited, intense ($10^{13} \text{ W cm}^{-2}$) femtosecond laser pulse at $800 \pm 8 \text{ nm}$.

ethylbenzene ($\text{C}_6\text{H}_5\text{CH}_3^+ = m/z = 92$ and $\text{C}_6\text{H}_5\text{C}_2\text{H}_5^+ = m/z = 106$) are situated in close proximity to the $\text{M}-(\text{OCH}_3)^+$ and $\text{M}-(\text{CH}_3)^+$ fragments of DMMP, as shown in figure 5(b). Naphthalene has a high fragmentation probability [33] in a strong femtosecond laser field, which results in extensive fragmentation throughout the entire TOF mass spectrum as shown in figure 5(a). The water molecules in the sample matrix do not create a complex background for our detection scheme since there is about $8 \mu\text{s}$ separation between arrival time of the H_2O^+ ion and the DMMP fragments of interest. Thus, unlike many other detection schemes the presence of water does not interfere with the target DMMP fragments ($\text{M}-(\text{OCH}_3)^+$, $\text{M}-2(\text{CH}_3)^+$ and $\text{M}-(\text{CH}_3)^+$).

To demonstrate active manipulation of the mass spectral fragmentation distribution, enhancement of the ratio of $\text{M}-2(\text{CH}_3)^+/\text{M}-(\text{CH}_3)^+$ was first specified as the control objective. Figure 6(a) reveals that the ratio of $\text{M}-2(\text{CH}_3)^+/\text{M}-(\text{CH}_3)^+$ could be enhanced by a factor of 5 in comparison with that obtained using the transform-limited laser pulse. The averaged mass spectrum obtained in the 30th generation (figure 7(b)) displays the optimized ratio of $\text{M}-2(\text{CH}_3)^+/\text{M}-(\text{CH}_3)^+$. These results suggest that at least two ‘sensor’ pulses exist for DMMP. In other words, there exist two laser pulse shapes having markedly different fragmentation distributions for DMMP. This variability occurs through a time-dependent, strong field manipulation of the molecular Hamiltonian. To demonstrate that additional sensor pulses exist, further experiments included manipulating the branching ratios of $\text{M}-(\text{OCH}_3)^+/\text{M}-(\text{CH}_3)^+$ and $\text{M}-(\text{OCH}_3)^+/\text{M}-2(\text{CH}_3)^+$, as shown in figure 6(b) and (c) with corresponding averaged mass spectra shown in figure 7(c) and (d), respectively. As seen in figure 6, the optimum ratio was achieved in the first ten generations (400 experiments) of the closed-loop evolutionary algorithm in all three discrimination experiments.

In each case, the adaptive algorithm increases monotonically to the optimal solution. The ability to control the fragmentation branching ratios in the mass

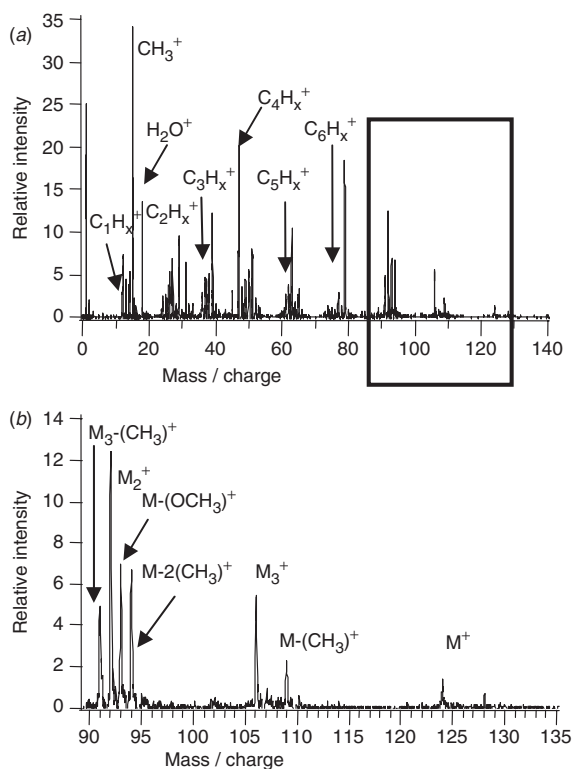


Figure 5. (a) The time-of-flight mass spectra for the mixture of dimethyl methylphosphonate, toluene, ethyl benzene, naphthalene, and water after excitation using a transform-limited, intense ($10^{13} \text{ W cm}^{-2}$) femtosecond pulse at $800 \pm 8 \text{ nm}$, the strong field excitation of naphthalene results in extensive fragmentation of the molecule denoted as C_1H_x^+ , C_2H_x^+ , C_3H_x^+ , C_4H_x^+ , C_5H_x^+ , and C_6H_x^+ . (b) A magnified view (from $m/z = 90$ to $m/z = 135$) of the spectrum that includes the parent ions of dimethyl methylphosphonate (M^+ ; $m/z = 124$), toluene (M_2^+ ; $m/z = 92$), ethyl benzene (M_3^+ ; $m/z = 106$), and naphthalene (M_4^+ ; $m/z = 128$) as well as the fragmented ions of dimethyl methylphosphonate.

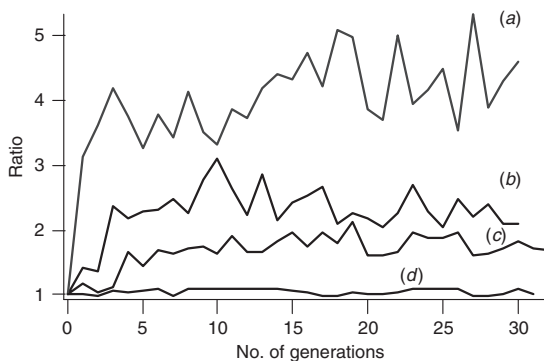


Figure 6. The ion ratio (fitness) as a function of a generation for (a) $\text{M-2(CH}_3\text{)}^+/\text{M-(CH}_3\text{)}^+$; (b) $\text{M-(OCH}_3\text{)}^+/\text{M-(CH}_3\text{)}^+$; (c) $\text{M-(OCH}_3\text{)}^+/\text{M-2(CH}_3\text{)}^+$; (d) ratios (a), (b) and (c) with the transform-limited pulse.

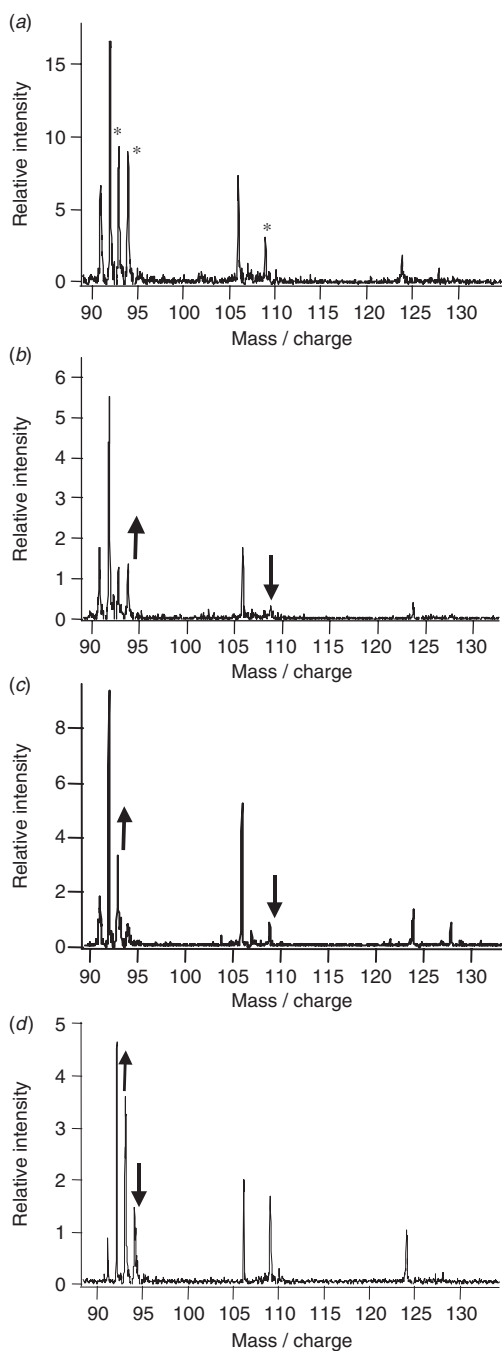


Figure 7. The averaged TOF mass spectrum obtained (a) with the transform-limited laser pulses (b) in the 30th generation for the maximization of $M-2(\text{CH}_3)^+ / M-(\text{CH}_3)^+$; (c) in the 30th generation for the maximization of $M-(\text{OCH}_3)^+ / M-(\text{CH}_3)^+$; (d) in the 30th generation for the maximization of $M-(\text{OCH}_3)^+ / M-2(\text{CH}_3)^+$.

spectrum of DMMP is specific to the details of the molecule's quantum mechanical Hamiltonian and the interaction with the intense laser pulse. Although the Hamiltonian is (generally) not known for such polyatomic systems, the closed-loop evolutionary process is capable of selectively finding an appropriate time-dependent electric field to manipulate the desired branching ratio, even in the presence of interferences.

In practice, selective alteration of the fragmentation distribution of a complex polyatomic molecule represents a new way to discriminate molecular identity [25]. The objective in these experiments is not to project the laser–molecule interaction onto a single observable for the system, such as the retention time in gas chromatography or the fragmentation distribution of a single mass spectrum. Rather, we used the entire laser–molecule interaction Hamiltonian to manipulate the projection of the system onto a number of final state channels. Such control provides dynamic discrimination method in two senses. First, the shaped, intense laser field alters the molecular Hamiltonian in a time-dependent manner [25] and thus, detected distribution. Active manipulation of the target species rather than passive detection is a new capability for sensing and signal processing. Second, a series of such laser pulses can be used to produce a series of fragmentation distributions. Thus, we can facilitate identification of a molecule through application of a series of specific strong field sensor pulses.

4. Conclusion

The mass spectral fragmentation/ionization distribution of the organophosphate DMMP was manipulated in the presence of a high background contributed by hydrocarbon and water in the detection scheme. We demonstrate the selective manipulation of three ion ratios, $(M-(OCH_3)^+/M-(CH_3)^+)$, $(M-2(CH_3)^+/M-(CH_3)^+)$ and $(M-(OCH_3)^+/M-2(CH_3)^+)$, to demonstrate a new type of chemically specific discrimination method for the identification of complex molecules. This novel sensing technology should have a wide variety of applications.

Acknowledgements

The authors wish to acknowledge the Department of Defense MURI Program, as managed by the Army Research Office, for financial support, and also George Heck for assistance with these experiments.

References

- [1] G.B. Koelle and J.A.F. Compton, *Military Chemical and Biological Agents: Chemical and Toxicological Properties* (Telford Press, NJ, Caldwell, 1987).
- [2] B. Ballantyne and T.C. Marrs, *Pharmacology and Toxicology of Organophosphates* (Butterworth-Heinemann, Oxford, 1992), pp. 35–39.

- [3] M. Fox and D. Scott, *Mutat. Res.* **75** 131 (1980).
- [4] J. Emsley and D. Hall, *Chemistry of Phosphorus: Environmental, Organic, Inorganic, Biochemical, and Spectroscopic Aspects* (Wiley, New York, 1976), p. 563.
- [5] H. Sohn and J. Steinhilber, *IJIMS* **1** 1 (1998).
- [6] M.S. Nieuwenhuizen and J.L.N. Harteveld, *Sensor Actuat. B Chem.* **40** 167 (1997).
- [7] D. Williams and G. Pappas, *Field Anal Chem. Tech.* **3** 45 (1999).
- [8] Y. Xie and B. Popov, *Anal. Chem.* **72** 2075 (2000).
- [9] S. Kumaran and M. Morita, *Talanta* **42** 649 (1995).
- [10] K.E. LeJeune, J.R. Wild and A.J. Russell, *Nature* **395** 27 (1998).
- [11] H. Sohn, S. Letant, M. Sailor, *et al.*, *J. Am. Chem. Soc.* **122** 5399 (2000).
- [12] S. Zhang and T. Swager, *J. Am. Chem. Soc.* **125** 3420 (2003).
- [13] M. Nagao, T. Takatori, Y. Matsuda, *et al.*, *J. Chromatogr. B* **701** 9 (1997).
- [14] Y. Matsuda, M. Nagao, T. Takatori, *et al.*, *Toxicol. Appl. Pharm.* **150** 310 (1998).
- [15] P. D'Agostino, L. Provost and P. Brooks, *J. Chromatogr.* **541** 121 (1991).
- [16] R.M. Black and R.W. Read, *J. Chromatogr. A* **794** 233 (1998).
- [17] M.C. Roch, L.W. Unger, R.N. Zare, *et al.*, *Anal. Chem.* **59** 1056 (1987).
- [18] E.S. Wes, H.C. Brian, E.H. Paul, *et al.*, *Anal. Chem.* **75** 6068 (2003).
- [19] E.S. Wes, H.C. Brian, E.H. Paul, *et al.*, *Anal. Chem.* **77** 4792 (2005).
- [20] C.E. Kientz, *J. Chromatogr. A* **814** 1 (1998).
- [21] V.D. Berkout, R.J. Cotter and D.P. Segers, *Am. Soc. Mass Spec.* **12** 641 (2001).
- [22] M. Noami, M. Kataoka and Y. Seto, *Anal. Chem.* **74** 4709 (2002).
- [23] D.B. Mark, R.C. William and R.W. Barry, *J. Chromatogr. A* **883** 185 (2000).
- [24] R.J. Levis and M.J. DeWitt, *J. Phys. Chem. A* **103** 6493 (1999).
- [25] R.J. Levis and H.A. Rabitz, *J. Phys. Chem.* **106** 6427 (2002).
- [26] R. Itakura, K. Yamanouchi, T. Tanabe, *et al.*, *J. Chem. Phys.* **119** 4179 (2003).
- [27] M.M. Wefers and K.A. Nelson, *Opt. Lett.* **18** 2032 (1993).
- [28] A.M. Weiner, *Rev. Sci. Instrum.* **71** 1929 (2000).
- [29] A. Assion, T. Baumert, M. Bergt, *et al.*, *Science* **282** 919 (1998).
- [30] R.J. Levis, G.M. Menkir and H. Rabitz, *Science* **292** 709 (2001).
- [31] D. Goldberg, *Genetic Algorithms in Search, Optimization and Machine Learning* (Addison-Wesley, Reading, MA, 1989).
- [32] R. Judson and H. Rabitz, *Phys. Rev. Lett.* **68** 1500 (1992).
- [33] M.J. Dewitt and R.J. Levis, *J. Chem. Phys.* **110** 11368 (1999).